

# Development and Numerical Solution of Integral Equations for Electromagnetic Scattering from a Trough in a Ground Plane

William D. Wood, Jr., and Aihua W. Wood

**Abstract**—We develop a set of scalar integral equations that govern the electromagnetic scattering from a two-dimensional (2-D) trough in an infinite perfectly conducting ground plane. We obtain accurate and efficient numerical solution to these equations via the method of moments (MoM). Our numerical implementation compares favorably to popular methods such as the finite element/boundary integral (FE/BI) method, generalized network formulation (GNF), and electric field integral equation (EFIE) techniques.

**Index Terms**—Electromagnetic scattering, ground plane.

## I. INTRODUCTION

INTEGRAL equations have been used in a variety of ways to formulate the scattering from an indentation in a perfectly conducting ground plane. The first and most widely used technique, the generalized network formulation (GNF) proposed by Harrington and Mautz [1], is based on the surface equivalence principle, in turn based on the vector Green's theorem [2]. The GNF is relatively simple to derive and implement, but it suffers from the problem of spurious resonances at the eigenfrequencies of the indentation. This phenomenon has been noted by several authors [3]–[5]. Hansen and Yaghjian [6] studied low-frequency scattering from a two-dimensional (2-D) trough in a ground plane, but their results are not applicable to resonant-sized and larger troughs. For large cavities, ray-based methods have been employed [7], [8], but are not valid for resonant-sized and smaller geometries. Finally, field-iterative methods [9], [10] have been pursued for large cavity scattering problems, but their accuracy is questionable for resonant-sized geometries.

Asvestas and Kleinman [11] developed a set of coupled vector integral equations for a three-dimensional (3-D) unfilled cavity-backed aperture in a perfectly conducting ground plane. They claimed, but did not prove that these integral equations are uniquely solvable at all frequencies. Recently, this approach was generalized to handle cavities filled with a homogeneous material [12]. In this paper, we derive a related set of coupled scalar integral equations for a material-filled 2-D trough in a ground plane. We also present numerical results

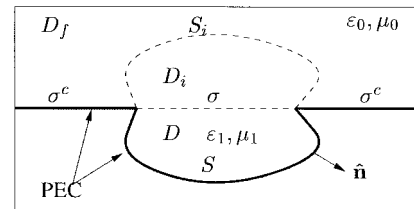


Fig. 1. The geometry of a cavity-backed aperture. The figure shows a 2-D cross-sectional view, with regions and surfaces defined.  $\sigma$  and  $\sigma^c$  lie in the  $xy$ -plane, and free-space comprises the half-space  $Z > 0$ .

that show these integral equations are immune to spurious resonances.

We organize the paper as follows. In Section II, we introduce the geometry and define the basic quantities. In Section III, we derive the scalar integral equations. Finally, in Sections IV and V, we present our numerical implementation and results and compare them to those of hybrid finite element/boundary integral (FE/BI), GNF, and electric field integral equation (EFIE) techniques.

## II. NOTATIONS & CONVENTIONS

The geometry is shown in Fig. 1. The aperture  $\sigma$ , its complement in the  $xy$ -plane  $\sigma^c$ , the cavity surface  $S$ , and the cavity volume  $D$  are defined as in [11]. The subscript  $i$  on a quantity denotes its image across the ground plane. The upper half-space is filled with free-space while  $D$  is filled with material characterized by constant scalar permittivity  $\epsilon_1$  and permeability  $\mu_1$ .

Known incident fields  $\vec{E}^{\text{inc}}$  and  $\vec{H}^{\text{inc}}$  impinge on the open cavity, giving rise to the scattered fields  $\vec{E}^{\text{scat}}$  and  $\vec{H}^{\text{scat}}$  and the reflected fields  $\vec{E}^{\text{ref}}$  and  $\vec{H}^{\text{ref}}$  (the fields scattered by an unbroken ground plane). The scattered fields represent a perturbation due to the presence of the cavity. The fields satisfy the same boundary and radiation conditions as in [11]. In addition, we note that the tangential field components are continuous across  $\sigma$ .

We employ the half-space 3-D scalar Green's functions defined in [11], altered for the  $\exp(j\omega t)$  time convention. That is,  $G_D = G(\vec{r}, \vec{r}') - G(\vec{r}, \vec{r}'_i)$  and  $G_N = G(\vec{r}, \vec{r}') + G(\vec{r}, \vec{r}'_i)$ , with  $G(\vec{r}, \vec{r}') = \exp(-jkR)/(4\pi R)$ , and  $R = |\vec{r} - \vec{r}'|$ . Paralleling [11], we define the dyadic functions  $\bar{\bar{I}} = -jk\nabla G \times \bar{\bar{I}}$ ,  $\bar{\bar{I}}_1 = -jk(\nabla G_N \times \bar{\bar{I}}_t + \nabla G_D \times \hat{z}\hat{z})$  and  $\bar{\bar{I}}_2 = -jk(\nabla G_D \times \bar{\bar{I}}_t + \nabla G_N \times \hat{z}\hat{z})$ , with  $\bar{\bar{I}} = \hat{x}\hat{x} + \hat{y}\hat{y} + \hat{z}\hat{z}$

Manuscript received January 26, 1998; revised July 22, 1998.

W. D. Wood, Jr., is with the Electromagnetics Division, Air Force Research Laboratory, Wright-Patterson AFB, OH 45433-7602 USA.

A. W. Wood is with the Department of Mathematics and Statistics, Air Force Institute of Technology, Wright-Patterson AFB, OH 45433-7765 USA.

Publisher Item Identifier S 0018-926X(99)07960-0.

and  $\bar{\mathbf{I}}_t = \hat{x}\hat{x} + \hat{y}\hat{y}$ . We note that these equations are valid in two dimensions if we make use of the identity

$$\int_{-\infty}^{\infty} \frac{e^{-jkR}}{4\pi R} dz = \frac{1}{4j} H_0^{(2)}(k|\bar{\rho} - \bar{\rho}'|) \equiv G^{(2D)}(\bar{\rho}, \bar{\rho}') \quad (1)$$

where  $H_0^{(2)}$  is the Hankel function of the second kind and  $\bar{\rho} = \bar{\mathbf{r}} \cdot \bar{\mathbf{I}}_t$ .

### III. THEORY AND APPLICATIONS

In this section, we present our main theorems.

*Theorem 1:* Let  $V$  be a cylinder parallel to  $\hat{x}$  with cross section  $D \subset \mathbf{R}^2$ . Assume that  $\partial D$  is piecewise smooth. Let  $\hat{\mathbf{n}}$  be the outward unit normal vector on  $\partial D$  and  $G = G^{(2D)}$ . If  $\bar{\mathbf{A}} = \bar{\mathbf{A}}(y, z)$  satisfies the homogeneous wave equation  $\forall \bar{\mathbf{r}} \in D$ , then

$$\int_{\partial D} \hat{\mathbf{n}} \cdot [\bar{\mathbf{A}} \times (\nabla \times \bar{\Gamma}) + (\nabla \times \bar{\mathbf{A}}) \times \bar{\Gamma}] dl = \begin{cases} jk\nabla' \times \bar{\mathbf{A}}(\bar{\mathbf{r}}') & \bar{\mathbf{r}}' \in D \\ 0 & \bar{\mathbf{r}}' \notin \bar{D}. \end{cases} \quad (2)$$

*Proof:* Restrict  $x' = 0$  so that  $\bar{\mathbf{r}}'$  lies in the  $yz$ -plane. Let  $V = \{(x, y, z) | (y, z) \in D, -\infty < x < \infty\}$ . Denote  $f = \hat{\mathbf{n}} \cdot [\bar{\mathbf{A}} \times \bar{\Gamma}^{(3D)} + (\nabla \times \bar{\mathbf{A}}) \times \bar{\Gamma}^{(3D)}]$ . By (17) of [12],

$$\int_{\partial V} f ds = \lim_{X \rightarrow \infty} \left( \int_{-X}^X \int_{\partial D} f dl dx + \int_{(D, -X)} f dl + \int_{(D, X)} f dl \right) \equiv I_1 + I_2 + I_3$$

which equals the right-hand side of (2). Since  $\bar{\mathbf{A}} \in C^1(V)$  and  $G \sim 1/|x|$  as  $|x| \rightarrow \infty$ , it is easy to show that  $I_2 = I_3 = 0$ . On the other hand

$$\begin{aligned} I_1 &= \int_{-\infty}^{\infty} \int_{\partial D} f dl dx = \int_{\partial D} \int_{-\infty}^{\infty} f dx dl \\ &= -jk \int_{\partial D} \hat{\mathbf{n}} \cdot \left\{ \bar{\mathbf{A}} \times \left[ \nabla \times \left( \nabla \int_{-\infty}^{\infty} G^{(3D)} dx \times \bar{\Gamma} \right) \right] \right. \\ &\quad \left. + (\nabla \times \bar{\mathbf{A}}) \times \left( \nabla \int_{-\infty}^{\infty} G^{(3D)} dx \times \bar{\Gamma} \right) \right\} dl \\ &= -jk \int_{\partial D} \hat{\mathbf{n}} \cdot \left\{ \bar{\mathbf{A}} \times [\nabla \times (\nabla G^{(2D)} \times \bar{\Gamma})] \right. \\ &\quad \left. + (\nabla \times \bar{\mathbf{A}}) \times (\nabla G^{(2D)} \times \bar{\Gamma}) \right\} dl \\ &= \int_{\partial D} \hat{\mathbf{n}} \cdot [\bar{\mathbf{A}} \times (\nabla \times \bar{\Gamma}^{(2D)}) + (\nabla \times \bar{\mathbf{A}}) \times \bar{\Gamma}^{(2D)}] ds \end{aligned}$$

which is the left-hand side of (2) and thus completes the proof.  $\square$

*Theorem 2:* Under the same conditions on  $D$  and  $\bar{\mathbf{A}}$  as in Theorem 1, the following identity holds:

$$\int_{\partial D} \hat{\mathbf{n}} \cdot [\bar{\mathbf{A}} \times (\nabla \times \bar{\Gamma}_m^{(2D)}) + (\nabla \times \bar{\mathbf{A}}) \times \bar{\Gamma}_m^{(2D)}] dl = \begin{cases} jk\nabla' \times \bar{\mathbf{A}}(\bar{\mathbf{r}}') & \bar{\mathbf{r}}' \in D \\ (-1)^{m+1} jk\nabla'_i \times \bar{\mathbf{A}}'(\bar{\mathbf{r}}'_i) & \bar{\mathbf{r}}' \in D_i \\ 0 & \bar{\mathbf{r}}' \notin \bar{D} \cup \bar{D}_i. \end{cases} \quad (3)$$

where  $m = 1, 2$ .

The proof of Theorem 2 is similar to that of Theorem 1 and is omitted here for brevity.

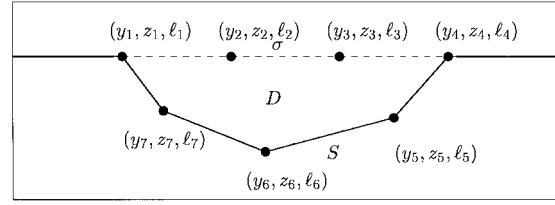


Fig. 2. A discretized trough geometry. The aperture  $\sigma$  (dashed line) is partitioned into  $N_1$  line segments, while the trough surface  $S$  (solid line) is partitioned into  $N_2$  line segments. In this figure,  $N_1 = 3$  and  $N_2 = 4$ .

*Theorem 3:* Let  $D$  and  $\bar{\mathbf{A}}$  be as in Theorem 1. Then the following identity holds:

$$\lim_{\bar{\mathbf{r}}' \rightarrow \bar{\mathbf{r}}} \hat{\mathbf{n}} \times \int_{\partial D} \bar{\mathbf{A}}(\bar{\mathbf{r}}') \cdot \bar{\Gamma}(\bar{\mathbf{r}}', \bar{\mathbf{r}}) dl'' = \mp \frac{jk}{2} \bar{\mathbf{A}}(\bar{\mathbf{r}}) + \hat{\mathbf{n}} \times \int_{\partial D} \bar{\mathbf{A}}(\bar{\mathbf{r}}') \cdot \bar{\Gamma}(\bar{\mathbf{r}}', \bar{\mathbf{r}}) dl'' \quad (4)$$

where the upper sign is taken if  $\bar{\mathbf{r}}' \rightarrow \bar{\mathbf{r}}$  from the exterior of  $D$  and the lower sign from the interior.

The proof of Theorem 3 is a consequence of the theorem on page 205 of [13].

To apply the above theorems, we consider the cavity-backed aperture problem with the geometry of an infinite trough parallel to  $\hat{x}$  with cross section  $D$  bounded by  $\partial D = \sigma \cup S$  in the  $yz$ -plane, as shown in Fig. 2. Applying Theorems 1–3 to this problem, letting  $\bar{\mathbf{A}}$  be  $\bar{\mathbf{E}}$ ,  $\bar{\mathbf{H}}$ , and  $\bar{\mathbf{H}}^{\text{inc}}$  in turn, and using the boundary conditions satisfied by the fields as stated in Section II, we obtain

$$\begin{aligned} \hat{z} \times \int_{\sigma} \hat{z} \times \bar{\mathbf{H}}(\bar{\mathbf{r}}') \cdot \nabla \times \bar{\Gamma}|_{k=k_1} d\sigma + \hat{z} \\ \times \int_S \hat{\mathbf{n}} \times \bar{\mathbf{H}}(\bar{\mathbf{r}}') \cdot \nabla \times \bar{\Gamma}|_{k=k_1} dl \\ = \frac{-k_1^2 Y_1}{2} \hat{z} \times \bar{\mathbf{E}}(\bar{\mathbf{r}}') \quad \text{for } \bar{\mathbf{r}}' \in \sigma \end{aligned} \quad (5)$$

$$\begin{aligned} -\hat{z} \times \int_{\sigma} \hat{z} \times \bar{\mathbf{E}}(\bar{\mathbf{r}}') \cdot \left\{ \frac{\nabla \times \bar{\Gamma}}{-jk} \Big|_{k=k_1} - \frac{\nabla \times \bar{\Gamma}}{-jk_0} \Big|_{k=k_0} \right\} d\sigma \\ + \frac{jk_1 Z_1 + jk_0 Z_0}{2} \hat{z} + \bar{\mathbf{H}}(\bar{\mathbf{r}}') - Z_1 \hat{z} \\ \times \int_S \hat{\mathbf{n}} \times \bar{\mathbf{H}}(\bar{\mathbf{r}}') \cdot \bar{\Gamma}|_{k=k_1} dl \\ = jk_0 Z_0 \hat{z} \times \bar{\mathbf{H}}^{\text{inc}}(\bar{\mathbf{r}}') \quad \text{for } \bar{\mathbf{r}}' \in \sigma \end{aligned} \quad (6)$$

and

$$\begin{aligned} 2\hat{\mathbf{n}}' \times \int_{\sigma} \hat{z} \times \bar{\mathbf{H}}(\bar{\mathbf{r}}') \cdot \bar{\Gamma}|_{k=k_1} d\sigma + \hat{\mathbf{n}}' \\ \times \int_S \hat{\mathbf{n}} \times \bar{\mathbf{H}}(\bar{\mathbf{r}}') \cdot \bar{\Gamma}|_{k=k_1} dl \\ = \frac{jk_1}{2} \hat{\mathbf{n}} \times \bar{\mathbf{H}}(\bar{\mathbf{r}}') \quad \text{for } \bar{\mathbf{r}}' \in S \end{aligned} \quad (7)$$

where  $Z_1 = 1/Y_1 = \sqrt{\mu_i/\epsilon_1}$ ,  $i = 0, 1$ .

We now derive scalar equations under TM polarization.<sup>1</sup> Let  $\bar{\mathbf{E}}(y, z) = u(y, z)\hat{x}$  and  $\bar{\mathbf{E}}^{\text{inc}}(y, z) = e^{jk_0(y \sin \theta + z \cos \theta)}\hat{x}$ .

<sup>1</sup> Scalar equations can be derived in a similar manner under TE polarization. Here, for brevity, we only demonstrate the TM polarization.

Then  $\vec{H}(y, z) = -(1/jkZ)\nabla u \times \hat{x}$  and  $\vec{H}^{\text{inc}}(y, z) = Y_0(-\hat{y} \cos \theta + \hat{z} \sin \theta)e^{jk_0(y \sin \theta + z \cos \theta)}\hat{x}$ . Then  $\vec{H}(y, z) = -(1/jkZ)\nabla u \times \hat{x}$  and  $\vec{H}^{\text{inc}}(y, z) = Y_0(-\hat{y} \cos \theta + \hat{z} \sin \theta)e^{jk_0(y \sin \theta + z \cos \theta)}$ , where  $\theta$  is the angle between the positive  $z$ -axis and the propagation direction of the incident field.

Correspondingly, we have

$$\begin{aligned} \hat{n} \times \vec{H}(\vec{r}') &= \frac{1}{jk_1 Z_1} \frac{\partial u}{\partial n} \hat{x}, & \vec{r}' \in S \\ \hat{z} \times \vec{H}(\vec{r}') &= \frac{1}{jk_1 Z_1} \frac{\partial u}{\partial z} \hat{x}, & \vec{r}' \in \sigma \end{aligned} \quad (8)$$

$$\begin{aligned} \hat{z} \times \vec{E}(\vec{r}') &= u(\vec{r}')\hat{y}, & \vec{r}' \in \sigma \\ \hat{z} \times \vec{H}^{\text{inc}}(\vec{r}') &= Y_0 \cos \theta e^{jk_0 y \sin \theta} \hat{x}, & \vec{r}' \in \sigma \end{aligned} \quad (9)$$

Substitute (8) and (5) to get a scalar equation. But first, we consider  $\nabla \times \vec{G} = -jk(k_1^2 \vec{G} + \nabla \nabla G)$  for  $\vec{r}, \vec{r}' \in \sigma$ . Note that  $\nabla \nabla G$  has only  $\hat{y}$  and  $\hat{z}$  components, while  $\hat{z} \times \vec{H}$  is  $\hat{x}$  directed, so we have  $\hat{n} \times \vec{H} \cdot \nabla \nabla G = 0, \forall \vec{r}' \in \sigma$ . Thus, the left side of (5) reduces to  $-(k_1^2/Z_1) \int_{\partial D} G(\partial u/\partial u) dl \hat{y}$ , while the right-hand side of (5) is  $(-k_1^2/2Z_1)u\hat{y}$ . Hence, we obtain

$$\int_{\partial D} \frac{\partial u(\vec{r}')}{\partial n} G_1 dl = \frac{1}{2} u(\vec{r}') \quad \text{for } \vec{r}' \in \sigma \quad (10)$$

where  $G_m = G|_{k=k_m}, m = 0, 1$ . Similarly, we substitute (8) into (6) and (7) and obtain the remaining scalar equations

$$\begin{aligned} \int_{\sigma} u(\vec{r}') \left[ k_1^2 G_1 - k_0^2 G_0 + \frac{\partial^2 (G_1 - G_0)}{\partial y^2} \right] d\sigma \\ + \frac{1}{2} \left( 1 + \frac{\mu_0}{\mu_1} \right) \frac{\partial u(\vec{r}')}{\partial z} - \int_S \frac{\partial u(\vec{r}')}{\partial n} \frac{\partial G_1}{\partial z} ds \\ = jk_0 \cos \theta e^{jk_0 y' \sin \theta} \quad \text{for } \vec{r}' \in \sigma \end{aligned} \quad (11)$$

and

$$\begin{aligned} 2 \int_{\sigma} \frac{\partial u(\vec{r}')}{\partial z} \hat{n}' \cdot \nabla G d\sigma + \int_S \frac{\partial u(\vec{r}')}{\partial z} \\ \cdot \left( n'_y \frac{\partial G_N}{\partial y} + n'_z \frac{\partial G_D}{\partial z} \right) ds \\ = \frac{-1}{2} \frac{\partial u(\vec{r}')}{\partial n} \quad \text{for } \vec{r}' \in S. \end{aligned} \quad (12)$$

#### IV. NUMERICAL SOLUTION

In this section, we employ the method of moments (MoM) [14] to find an approximate solution to (10)–(12). Pulse-basis functions and delta testing functions are used to reduce the complexity of the matrix element computations.

To demonstrate the MoM implementation of our problem, we present, without loss of generality, the approximation scheme for (10). We use the nodes  $(y_i, z_i, \ell_i)$  to denote the

$(y, z)$  coordinates and  $\ell$  the arc length of the nodes along the perimeter of the trough. Let there be  $N_1$  segments on the aperture  $\sigma$  and  $N_2$  on  $S$  as shown in Fig. 2. We define the two unknowns in (10)

$$\begin{aligned} \frac{\partial u(\ell)}{\partial n} &= \sum_{n=1}^{N_1+N_2} a_n p_n(\ell), & \vec{r}'(\ell) \in \sigma \cup S, & \quad \text{and} \\ u(\ell) &= \sum_{n=1}^{N_1} b_n p_n(\ell), & \vec{r}'(\ell) \in \sigma \end{aligned}$$

where the pulse function  $p_n(\ell)$  is unity for  $\ell_n \leq \ell \leq \ell_{n+1}$  and zero elsewhere. We use the delta testing functions  $w_m(\ell) = \delta(\ell - \ell_{m+(1/2)})$  where  $\ell_{m+(1/2)} = (\ell_m + \ell_{m+1})/2$ . Thus, (10) is discretized as

$$\sum_{n=1}^{N_1+N_2} a_n \int_{\ell_n}^{\ell_{n+1}} G_1(\ell, \ell') d\ell - \frac{1}{2} \sum_{n=1}^{N_1} b_n p_n(\ell') = 0.$$

Taking the inner product with the testing functions on both sides of the equation and using the sifting property of the delta function yields

$$\sum_{n=1}^{N_1+N_2} a_n \alpha_{mn} - \frac{1}{2} b_m = 0 \quad (13)$$

where  $\alpha_{mn} = \int_{\ell_n}^{\ell_{n+1}} G_1(\ell, \ell_{m+(1/2)}) d\ell$  and  $m = 1 \dots N_1$ . Using matrix notation we construct the equation at the bottom of the page. Similarly we produce  $A_2$  and  $A_3$  using (11) and (12), resulting in the matrix system  $Au = f$  where  $A = [A_1 \ A_2 \ A_3]^T, u = [a_1 \dots a_{N_1+N_2} \ b_1 \dots b_{N_1}]^T$  and  $f = [0 \dots 0 \ f_1 \dots f_{N_1} \ 0 \dots 0]^T$ . The nonzero elements of  $f$  are found by evaluating the right side of (11) at the match points. The matrix system may then be solved to find the expansion coefficients  $\{a_i\}_{i=1}^{N_1+N_2}$  and  $\{b_i\}_{i=1}^{N_1}$ .

#### V. NUMERICAL RESULTS

In this section, we present some numerical results for the case of an unfilled cavity; that is, where  $k_0 = k_1$ . The first experiment is for a rectangular trough and the results are compared to those from a hybrid FE/BI technique [15]. We also demonstrate the solvability of the problem using our formulation and compared it to the GNF approach. Our second experiment is for a V-shaped trough and the results are compared to the EFIE implementation [16].

##### A. Test Case I

We examine a rectangular trough, 1.2 m wide  $\times$  0.8 m deep, illuminated by a 300 MHz TM plane wave. We use ten pulses per wavelength, resulting in a  $28 \times 28$  matrix. These results

$$A_1 = \begin{bmatrix} \alpha_{11} & \alpha_{12} & \cdots & \alpha_{1N_1+N_2} & -\frac{1}{2} & 0 & \cdots & 0 \\ \alpha_{21} & \alpha_{22} & \cdots & \alpha_{2N_1+N_2} & 0 & -\frac{1}{2} & \cdots & 0 \\ \vdots & \vdots & \ddots & \vdots & \vdots & \vdots & \ddots & \vdots \\ \alpha_{N_1 1} & \alpha_{N_1 2} & \cdots & \alpha_{N_1 N_1+N_2} & 0 & 0 & \cdots & -\frac{1}{2} \end{bmatrix}$$

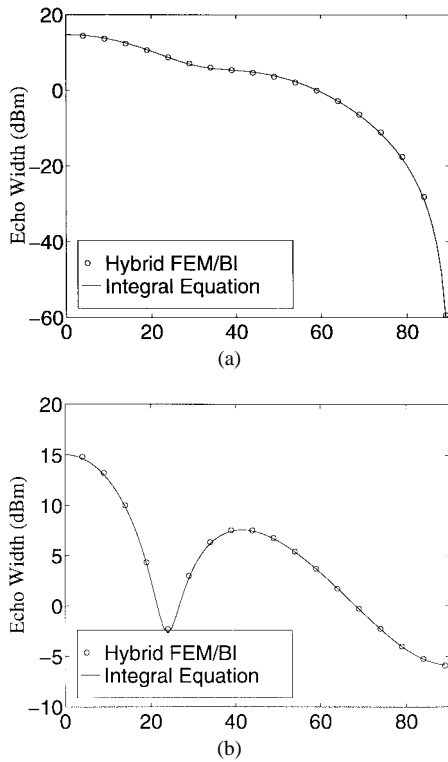


Fig. 3. Monostatic echo width vs. angle from normal for a rectangular trough with depth =  $0.8\lambda$  and width =  $1.2\lambda$ . (a)  $TM_x$  pol. (b)  $TE_x$  pol. Echo width is in units decibels relative to a 1-m isotropic scatterer (dBm).

are compared to the results of the FE/BI technique and are shown in Fig. 3.

This experiment shows an excellent agreement between the results produced by our integral equation method and that by the hybrid FE/BI technique; however, the latter involves meshing the entire cavity area and, thus, is much more computationally expensive than the former where only the perimeter of the cavity is discretized.

We note also that conventional integral equation based methods used to analyze a trough in a ground plane are based on the generalized network formulation [1] in which the scattering domain is partitioned into an interior region (the trough) and an exterior region (the half-space above the ground plane). An integral equation is written for each region separately and the two integral equations are coupled by enforcing field continuity across the aperture. An unfortunate byproduct of this partitioning scheme is the introduction of spurious resonances at frequencies corresponding to the cavity resonances of the interior region. At these frequencies, the generalized network formulation breaks down and the resulting coupled integral equations are not uniquely solvable. In the moment method, the presence of a spurious resonance manifests itself as an ill-conditioned impedance matrix.

We now demonstrate that the integral equations (10)–(12) are uniquely solvable even at frequencies which are troublesome for the GNF-based methods. The interior region is resonant at approximately 225 MHz, corresponding to the cutoff frequency of the  $TM_{11}$  and  $TE_{11}$  rectangular waveguide modes. Near this frequency, the condition number of the matrix for the interior region of the generalized network

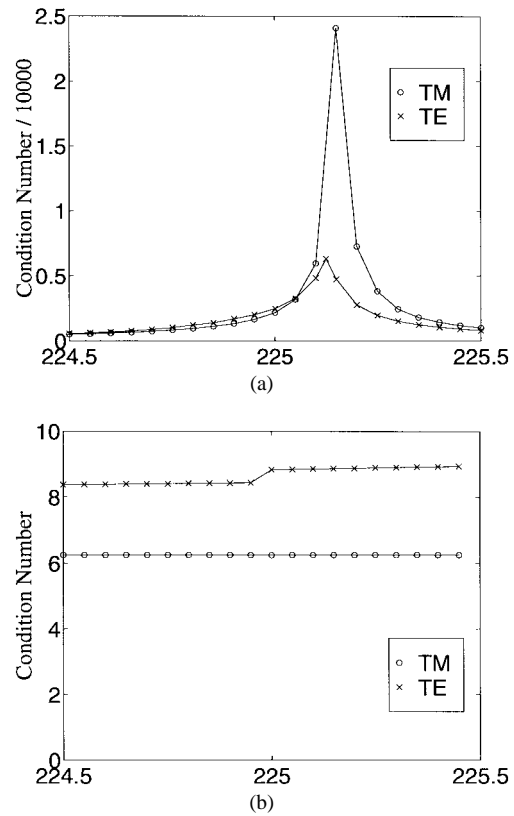


Fig. 4. Condition number versus frequency.

formulation becomes very high, as shown in Fig. 4(a). In contrast, the condition number for the matrix for the integral equations used here is very stable, as shown in Fig. 4(b). This is a direct result of our method of construction, which avoids the partitioning of the domain as is done in the GNF.

### B. Test Case II

We examine a V-shaped trough, 1.2 m wide  $\times$  0.8 m deep, illuminated by a 300 MHz TM plane wave. The geometry is illustrated in Fig. 5.

To implement the EFIE method to model a geometry involving an infinite ground plane, we employ vector background subtraction (VBS), a standard measurement technique.<sup>2</sup> We design a finite test body to mimic the infinite ground plane. To reduce the scattering from the test body, a  $2000 \Omega/\square$  resistive card of length 4 m is attached on each side of the perfect electric conductor to form a total length of 24 m. The results from both our integral equation method and the EFIE method are shown in Fig. 6. The oscillating effect evident in the EFIE approximation is a product of the interaction between the cavity and the edge (R-cards). In particular, the method fails near grazing incidence due to scattering from the bottom

<sup>2</sup>Vector background subtraction is a process to isolate the scattering due to a component of a larger body. First, the complex scattered field from the larger body with the component removed is determined. Then the complex scattered field from the larger body with the component installed is determined. The coherent difference between the two fields is attributed to the component alone. In actuality, the difference is the sum of direct scattering by the component and interactions between the component and the larger body. In many cases, the larger body is designed to minimize these interactions relative to the component scattering and so they may be neglected.

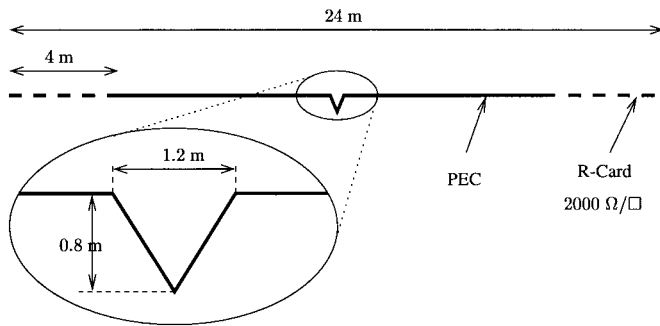


Fig. 5. Geometry of V-shaped trough. For the reference solution based on the EFIE, the ground plane is truncated. The edges of the finite ground plane are treated with  $2000 \Omega/\square$  R-Card to reduce the truncation effects.

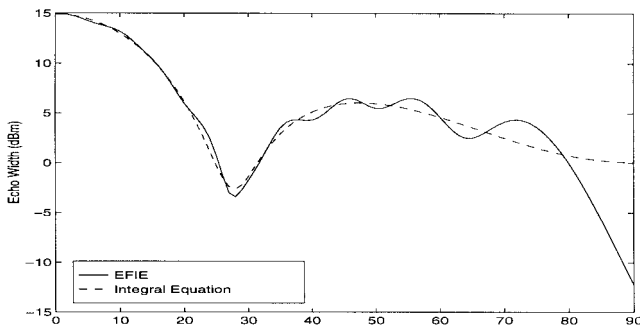


Fig. 6. RCS versus angle for V-shaped trough. The V-shaped trough illuminated by a 300-MHz plane wave incident from an angle  $\theta$ . The reference solution is from an EFIE-based moment method code, with the ground plane truncated. The effects of the truncated ground plane are evident in the oscillation seen in the reference solution caused by interactions between the trough and the truncation.

of the test fixture. However, the results from the new integral equations correctly predict the cavity scattering for all angles. This is due to the fact that the new integral equations are built on the Green's function for the conducting ground plane.

## VI. CONCLUSION

We have developed a set of coupled integral equations to describe the electromagnetic scattering from a material-filled trough in an infinite ground plane. The integral equations involve only the tangential field components on the bounding surface of the trough interior. The MoM is used to find a numerical solution to the integral equations when the trough is excited by an incident plane wave. The accuracy of the technique has been demonstrated through comparisons with other methods such as the GNF, hybrid FE/BI, and EFIE schemes. Furthermore, we have shown that the new integral equations are immune to the problem of nonuniqueness due to spurious resonances.

## ACKNOWLEDGMENT

The authors wish to thank two anonymous reviewers for their insightful comments and suggestions.

## REFERENCES

[1] R. F. Harrington and J. R. Mautz, "A generalized network formulation for aperture problems," *IEEE Trans. Antennas Propagat.*, vol. AP-24, pp. 870–873, Nov. 1976.

- [2] K.-M. Chen, "A mathematical formulation of the equivalence principle," *IEEE Trans. Microwave Theory Tech.*, vol. 37, p. 1576–1581, Oct. 1989.
- [3] S.-K. Jeng, "Scattering from a cavity-backed slit in a ground plane—TE case," *IEEE Trans. Antennas Propagat.*, vol. 38, pp. 1523–1529, Oct. 1990.
- [4] S.-K. Jeng and S.-T. Tzeng, "Scattering from a cavity-backed slit in a ground plane—TM case," *IEEE Trans. Antennas Propagat.*, vol. 39, pp. 661–663, May 1991.
- [5] P. M. Goggans and T. H. Shumpert, "Backscatter RCS for TE and TM excitations of dielectric-filled cavity-backed apertures in two-dimensional bodies," *IEEE Trans. Antennas Propagat.*, vol. 39, pp. 1224–1227, Aug. 1991.
- [6] T. B. Hansen and A. D. Yaghjian, "Low-frequency scattering from two-dimensional perfect conductors," *IEEE Trans. Antennas Propagat.*, vol. 40, pp. 1389–1402, Nov. 1992.
- [7] H. Ling, R.-C. Chou, and S.-W. Lee, "Shooting and bouncing rays: Calculating the RCS of an arbitrarily shaped cavity," *IEEE Trans. Antennas Propagat.*, vol. 37, pp. 194–205, Feb. 1989.
- [8] R. J. Burkholder, "Two ray shooting methods for computing the EM scattering by large open-ended cavities," *Comput. Phys. Communicat.*, vol. 68, pp. 353–365, Nov. 1991.
- [9] D. H. Reuster and G. A. Thiele, "A field iterative method for computing the scattered electric fields at the apertures of large perfectly conducting cavities," *IEEE Trans. Antennas Propagat.*, vol. 43, pp. 286–290, Mar. 1995.
- [10] P. K. Murthy, K. C. Hill, and G. A. Thiele, "A hybrid-iterative method for scattering problems," *IEEE Trans. Antennas Propagat.*, vol. AP-34, pp. 1173–1180, Oct. 1986.
- [11] J. S. Asvestas and R. E. Kleinman, "Electromagnetic scattering by indented screens," *IEEE Trans. Antennas Propagat.*, vol. 42, pp. 22–30, Jan. 1994.
- [12] W. D. Wood, Jr., "Electromagnetic scattering from a cavity in a ground plane: Theory and experiment," Ph.D. dissertation, Air Force Inst. Technol., Mar. 1997.
- [13] C. Müller, *Foundations of the Mathematical Theory of Electromagnetic Waves*. New York: Springer-Verlag, 1969.
- [14] R. F. Harrington, *Field Computation by Moment Methods*. New York: Macmillan, 1968.
- [15] J.-M. Jin and J. L. Volakis, "A finite-element-boundary integral formulation for scattering by three-dimensional cavity-backed apertures," *IEEE Trans. Antennas Propagat.*, vol. 39, pp. 97–104, Jan. 1991.
- [16] A. Maue, "On the formulation of a general scattering problem by means of an integral equation," *Z. Phys.*, vol. 126, no. 7, pp. 601–618, 1949.

**William D. Wood, Jr.**, was born in Fairfax, VA. He received the B.S.E.E. degree from the University of Arizona, Tucson, in 1985, and the M.S.E.E. and Ph.D. degrees from the Air Force Institute of Technology, Wright-Patterson AFB, OH, in 1990 and 1997, respectively.

A Major in the United States Air Force, he is currently assigned to the Signature Technology Office of the Air Force Research Laboratory at Wright-Patterson Air Force Base. His duties include research in computational electromagnetics and radar cross-section measurement techniques.

Dr. Wood, Jr., is a member of Tau Beta Pi and Eta kappa Nu.



**Aihua W. Wood** was born in Qingdao, China. She received the B.S. degree in mathematics from Beijing University, China, in 1984, and the M.S. and Ph.D. degrees in mathematics from the University of Connecticut, Storrs, in 1988 and 1990, respectively.

She is currently an Associate Professor of Mathematics at the Air Force Institute of Technology (AFIT), Wright-Patterson Air Force Base, OH. Her research interests include electromagnetic scattering from complex objects and semilinear elliptic partial differential equations. Prior to joining AFIT, she

was a member of the faculty at Pennsylvania State University, University Park, and the Naval Postgraduate School, Monterey, CA.

Dr. Wood is a member of the American Mathematical Society.